J|A|C|S ARTICLES

Published on Web 07/10/2009

High-Triplet-Energy Dendrons: Enhancing the Luminescence of Deep Blue Phosphorescent Iridium(III) Complexes

Shih-Chun Lo,[†] Ruth E. Harding,[‡] Christopher P. Shipley,[§] Stuart G. Stevenson,[‡] Paul L. Burn,*[,†] and Ifor D. W. Samuel*[,‡]

Centre for Organic Photonics & Electronics, The University of Queensland, School of Chemistry & Molecular Biosciences, QLD 4072, Australia, Organic Semiconductor Centre, SUPA, School of Physics & Astronomy, University of St Andrews, North Haugh, Fife, KY16 9SS, U.K., and Chemistry Research Laboratory, Department of Chemistry, University of Oxford, Mansfield Road, Oxford, OX1 3TA, U.K.

Received April 20, 2009; E-mail: p.burn2@uq.edu.au; idws@st-andrews.ac.uk

Abstract: Solution-processable blue phosphorescent emitters with high luminescence efficiency are highly desirable for large-area displays and lighting applications. This report shows that when a *fac*-tris[1-methyl-5-(4-fluorophenyl)-3-*n*-propyl-1*H*-[1,2,4]triazolyl]iridium(III) complex core is encapsulated by rigid high-triplet-energy dendrons, both the physical and photophysical properties can be optimized. The high-triplet-energy and rigid dendrons were composed of twisted biphenyl dendrons with the twisting arising from the use of tetrasubstituted branching phenyl rings. The blue phosphorescent dendrimer was synthesized using a convergent approach and was found to be solution-processable and to possess a high glass transition temperature of 148 °C. The dendrimer had an exceptionally high solution photoluminescence quantum yield (PLQY) of 94%, which was more than three times that of the simple parent core complex (27%). The rigid and high-triplet-energy dendrons were also found to control the intermolecular interactions that lead to the quenching of the luminescence in the solid state, and the film PLQY was found to be 60% with the emission having Commission Internationale de l'Eclairage coordinates of (0.16, 0.16). The results demonstrate that dendronization of simple chromophores can enhance their properties. Single layer neat dendrimer organic light-emitting diodes (OLEDs) had an external quantum efficiency (EQE) of 0.4% at 100 cd/m^2. Bilayer devices with an electron transport layer gave improved EQEs of up to 3.9%. Time-resolved luminescence measurements suggest that quenching of triplets by the electron transport layer used in the bilayer OLEDs limits performance.

Introduction

Organic light-emitting diodes (OLEDs)[1] based on luminescent heavy metal complexes are playing a key role in next generation flat panel displays and solid-state lighting. Phosphorescence from osmium(II), platinum(II), and in particular iridium(III) gives an advantage over fluorescent materials in that both the singlet and triplet excitons that form in a device can be captured and decay radiatively thus leading to higher efficiencies.[2] For example, OLEDs based on the green emissive *fac*-tris(2-phenylpyridyl)-iridium(III) (Irppy$_3$) have shown a nearly 100% internal quantum efficiency.[3] While OLEDs with red and green phosphorescent iridium(III) complexes have proved fairly straightforward to produce, the same cannot be said for saturated blue emissive materials. Highly luminescent deep blue phosphorescent materials with Commission Internationale de l'Eclairage (CIE) coordinates less than (0.20, 0.20) have proved a challenge. For full color displays and solid-state lighting based on OLED technology, it would be advantageous to have deep blue phosphorescent materials with high photoluminescence quantum yields. Early work on materials that emitted blue phosphorescence involved attaching fluorine substituents on the basic Irppy$_3$ structure[4] and then moved to heteroleptic complexes with high triplet energy[5] and/or strong ligand field ancillary ligands.[6] More recently homoleptic small molecule iridium(III) complexes based on carbene[7] or phenyl triazole ligands[8] with saturated blue emission have been reported. In the former case, judicious choice of host

[†] The University of Queensland.
[‡] University of St Andrews.
[§] University of Oxford.

(1) (a) Tang, C. W.; van Slyke, S. A. *Appl. Phys. Lett.* **1987**, *51*, 913. (b) Burroughes, J. H.; Bradley, D. D. C.; Brown, A. R.; Marks, R. N.; Mackay, K.; Friend, R. H.; Burn, P. L.; Holmes, A. B. *Nature* **1990**, *347*, 539. (c) Forrest, S. R. *Nature* **2004**, *428*, 911. (d) Holder, E.; Langeveld, B. M. W.; Schubert, U. S. *Adv. Mater.* **2005**, *17*, 1109. (e) Grimsdale, A. C.; Chan, K. L.; Martin, R. E.; Jokisz, P. G.; Holmes, A. B. *Chem. Rev.* **2009**, *109*, 897.

(2) (a) Baldo, M. A.; O'Brien, D. F.; You, Y.; Shoustikov, A.; Sibley, S.; Thompson, M. E.; Forrest, S. R. *Nature* **1998**, *395*, 151. (b) Baldo, M. A.; Thompson, M. E.; Forrest, S. R. *Nature* **2000**, *403*, 750. (c) Bernhard, S.; Gao, X. C.; Malliaras, G. G.; Abruña, H. D. *Adv. Mater.* **2002**, *14*, 433. (d) Brooks, J.; Babaya, T.; Lamansky, S.; Djurovich, P. I.; Tsyba, I.; Bau, R.; Thompson, M. E. *Inorg. Chem.* **2002**, *41*, 3055. (e) Ikai, M.; Tokito, S.; Sakamoto, Y.; Suzuki, T.; Taga, Y. *Appl. Phys. Lett.* **2001**, *79*, 156. (f) Gong, X.; Ma, W. L.; Ostrowski, J. C.; Bazan, G. C.; Moses, D.; Heeger, A. J. *Adv. Mater.* **2004**, *16*, 615.

(3) Adachi, C.; Baldo, M. A.; Thompson, M. E.; Forrest, S. R. *J. Appl. Phys.* **2001**, *90*, 5048.

(4) Adachi, C.; Kwong, R. C.; Djurovich, P.; Adamovich, V.; Baldo, M. A.; Thompson, M. E.; Forrest, S. R. *Appl. Phys. Lett.* **2001**, *79*, 2082.

has led to relatively efficient OLEDs with good CIE coordinates. A key aspect of these studies has been the focus on small molecules that require evaporation together with a host. This places strict requirements on the properties of the host including the ability to be evaporated, transport charge, and have a triplet energy sufficiently high so as to not quench the luminescence.[9] There is therefore a need for blue phosphorescent materials that can be processed from solution for use in displays and lighting applications.

One successful approach to solution processable phosphorescent materials has been the development of light-emitting dendrimers. Phosphorescent light-emitting dendrimers generally consist of a light-emitting core, dendrons (branches), and surface groups, with the last playing the dominant role in the processability of the materials. The dendrons that have been developed for phosphorescent light-emitting dendrimers have fallen into two categories: those that are electrically insulating[10] and merely play a structural role in controlling the intermolecular interactions of the core, and those that are electroactive.[11] In both cases the precise control over the intercore distances means that the emissive cores can be photophysically independent thus avoiding interactions that lead to the quenching of the luminescence.[12] However, the cores can still be sufficiently close to allow the necessary charge transport in a device. This has made it possible to use dendrimers to make highly efficient solution-processed OLEDs with a neat light-emitting dendrimer layer, avoiding the need for a host.[13] The lack of a host material is attractive, both from the point of view of simplifying device fabrication and because finding suitable hosts for deep blue emission is challenging. The development of deep blue phosphorescent dendrimers places additional requirements on the properties of the dendrons. In particular it is important that the triplet energy of the dendron is above that of the core chromophore. However, none of the dendrons reported thus far have been suitable for devices containing saturated blue emissive iridium(III) complexes either having too low a triplet energy leading to the quenching of the luminescence, or giving dendrimers with thermal properties not suitable for device fabrication.[14,15]

In this work we report the development of a new rigid high-triplet-energy dendron that can be used to give a solution-processable saturated blue phosphorescent dendrimer with a high photoluminescence quantum yield. We show that when twisted biphenyl-based dendrons are attached to the saturated blue emissive core, *fac*-tris[1-methyl-5-(4-fluorophenyl)-3-*n*-propyl-1*H*-[1,2,4]triazolyl]iridium(III) (**1** in Figure 1), the properties of the simple complex are significantly enhanced. We compare the properties of the dendrimer **1** with the core complex **2**, and dendrimers with simple biphenyl **3** or diphenylethylene **4** dendrons and the same surface groups (Figure 1), and show that not only are the photophysical properties improved but the physical properties are now suitable for device fabrication. Finally, we report the performance of single and bilayer devices and describe the next challenges in materials development required for efficient large-area devices containing solution-processed deep blue phosphorescent materials.

Results and Discussion

To achieve the desired processing, thermal and photophysical properties dendrimer **1** (Scheme 1) incorporates several important design features: first, the *fac*-tris[1-methyl-5-(4-fluorophenyl)-3-*n*-propyl-1*H*-[1,2,4]triazolyl]iridium(III) complex used as the core emits blue phosphorescence with CIE coordinates in solution of (0.16, 0.13). The photoluminescence (PL) peaks are at 428 and 456 nm,[8] which corresponds to energies of 2.9 and 2.7 eV, respectively. Second, the dendrons are composed of tetrasubstituted phenyl rings, ensuring that adjacent phenyl rings are twisted out of plane thus breaking the π-electron delocalization. Molecular orbital calculations show that the chromophores within the tetrasubstituted phenyl-based dendrons have triplet energies of 3.4 eV, which is 0.5 eV higher in energy than the emission of the core. The high triplet energy of the chromophores within the dendrons should ensure that the PL of the core is not quenched by the dendrons.[14] Third, the presence of the second generation and first generation dendrons attached to the triazolyl and phenyl rings of the ligands respectively, ensures that the emissive core is encapsulated by the dendrons thus protecting it from intermolecular interactions that can lead to quenching of the PL. Fourth, the rigid nature of the dendrons will provide for a high glass transition temperature (T_g), and finally, the 2-ethylhexyloxy surface groups ensure solubility and that good-quality spin-coated films can be formed.

Synthesis. Our synthetic route to the dendrons and dendrimer is shown in Scheme 1. The strategy involved the formation of the elaborated [1-methyl-5-(4-fluorophenyl)-3-*n*-propyl-1*H*-[1,2,4]triazolyl] ligand with three bromine groups (**19**) available for attachment to a first generation dendron **18** with a boronic acid at its focus.

We will first discuss the synthesis of the tribromo triazole ligand **19** and then the first generation boronic acid focused dendron **18** and finally the dendrimer formation. The key step in the synthe-

(5) (a) Holmes, R. J.; D'Andrade, B. W.; Forrest, S. R.; Ren, X.; Li, J.; Thompson, M. E. *Appl. Phys. Lett.* **2003**, *83*, 3818. (b) Li, J.; Djurovich, P. I.; Alleyne, B. D.; Yousufuddin, M.; Ho, N. N.; Thomas, J. C.; Peters, J. C.; Bau, R.; Thompson, M. E. *Inorg. Chem.* **2005**, *44*, 1713. (c) Coppo, P.; Plummer, E. A.; De Cola, L. *Chem. Commun.* **2004**, 1774. (d) Yang, C.-H.; Cheng, Y.-M.; Chi, Y.; Hsu, C.-J.; Fang, F.-C.; Wong, K.-T.; Chou, P.-T.; Chang, C.-H.; Tsai, M.-H.; Wu, C.-C. *Angew. Chem., Int. Ed.* **2007**, *46*, 2418. (e) Chang, C.-F.; Cheng, Y.-M.; Chi, Y.; Chiu, Y.-C.; Lin, C.-C.; Lee, G.-H.; Chou, P.-T.; Chen, C.-C.; Chang, C.-H.; Wu, C.-C. *Angew. Chem., Int. Ed.* **2008**, *47*, 4542.

(6) (a) Nazeeruddin, M. K.; Humphry-Baker, R.; Berner, D.; Rivier, S.; Zuppiroli, L.; Grätzel, M. *J. Am. Chem. Soc.* **2003**, *125*, 8790. (b) Dedeian, K.; Shi, J.; Forsythe, E.; Morton, D. C.; Zavalij, P. Y. *Inorg. Chem.* **2007**, *46*, 1603. (c) Di Censo, D.; Fantacci, S.; De Angelis, F.; Klein, C.; Evans, N.; Kalyanasundaram, K.; Bolink, H. J.; Grätzel, M.; Nazzeeruddin, M. K. *Inorg. Chem.* **2008**, *44*, 980.

(7) (a) Sajoto, T.; Djurovich, P. I.; Tamayo, A.; Yousufuddin, M.; Bau, R.; Thompson, M. E.; Holmes, R. J.; Forrest, S. R. *Inorg. Chem.* **2005**, *44*, 7992. (b) Holmes, R. J.; Forrest, S. R.; Saioto, T.; Tamayo, A.; Djurovich, P. I.; Thompson, M. E. *Appl. Phys. Lett.* **2005**, *87*, 243507.

(8) Lo, S.-C.; Shipley, C. P.; Bera, R. N.; Harding, R. E.; Cowley, A. R.; Burn, P. L.; Samuel, I. D. W. *Chem. Mater.* **2006**, *18*, 5119.

(9) (a) Tokito, S.; Iijima, T.; Suzuri, Y.; Kita, H.; Tsuzuki, T.; Sato, F. *Appl. Phys. Lett.* **2003**, *83*, 569. (b) Ren, X.; Li, J.; Holmes, R. J.; Djurovich, P. I.; Forrest, S. R.; Thompson, M. E. *Chem. Mater.* **2004**, *16*, 4743.

(10) Lo, S.-C.; Namdas, E. B.; Burn, P. L.; Samuel, I. D. W. *Macromolecules* **2003**, *36*, 9721.

(11) (a) Lo, S.-C.; Namdas, E. B.; Shipley, C. P.; Markham, J. P. J.; Anthopolous, T. D.; Burn, P. L.; Samuel, I. D. W. *Org. Electron.* **2006**, *7*, 85. (b) Knights, K. A.; Stevenson, S. G.; Shipley, C. P.; Lo, S.-C.; Olsen, S.; Harding, R. E.; Gambino, S.; Burn, P. L.; Samuel, I. D. W. *J. Mater. Chem.* **2008**, *18*, 2121.

(12) (a) Adronov, A.; Fréchet, J. M. J. *Chem. Commun.* **2000**, 1701. (b) Lo, S.-C.; Burn, P. L. *Chem. Rev.* **2007**, *107*, 1097. (c) Burn, P. L.; Lo, S.-C.; Samuel, I. D. W. *Adv. Mater.* **2007**, *19*, 1675.

(13) Lo, S.-C.; Anthopoulos, T. D.; Namdas, E. B.; Burn, P. L.; Samuel, I. D. W. *Adv. Mater.* **2005**, *17*, 1945.

(14) Lo, S.-C.; Bera, R. N.; Harding, R. E.; Burn, P. L.; Samuel, I. D. W. *Adv. Funct. Mater.* **2008**, *18*, 3080.

(15) Lo, S.-C.; Harding, R. E.; Brightman, E.; Burn, P. L.; Samuel, I. D. W. *J. Mater. Chem.* **2009**, *19*, 3213.

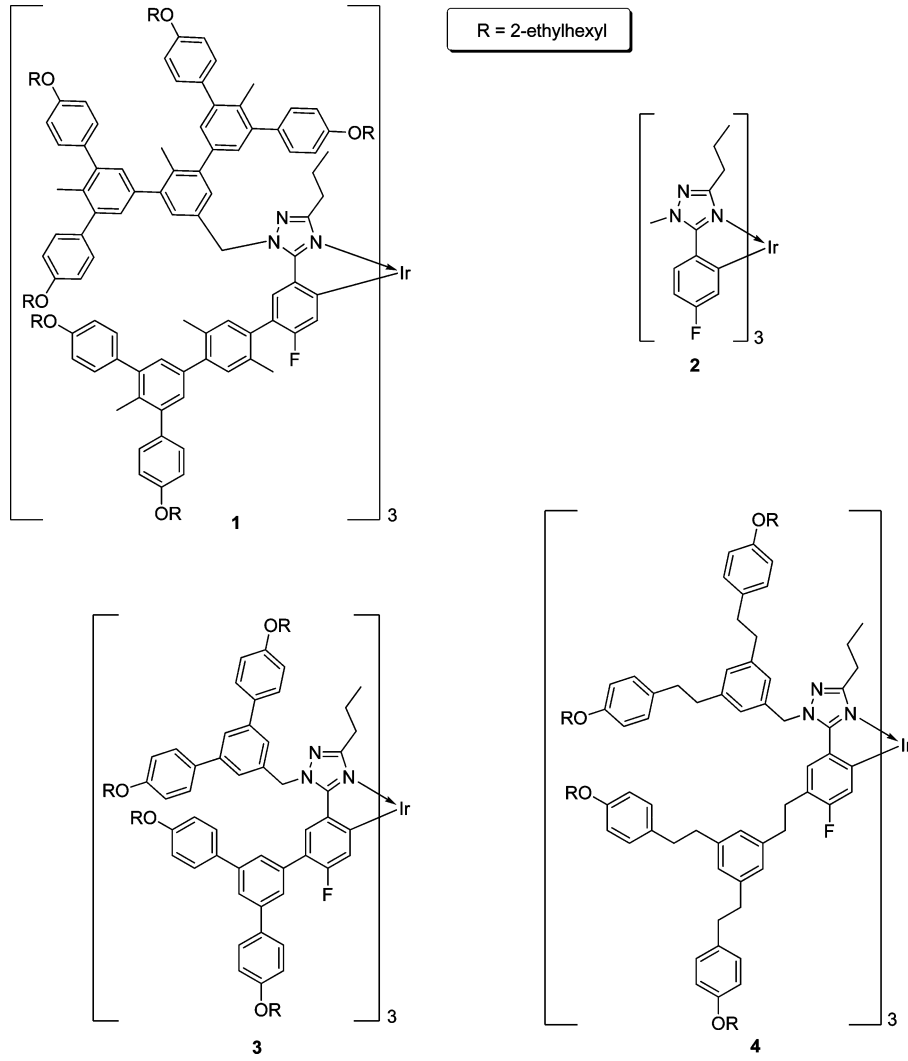

Figure 1. Chemical structures of the parent iridium(III) complex **2**, and dendrimers **1**, **3**, and **4**.

sis of **19** was the reaction of the benzylhydrazine **8** with the butanimidic acid ethyl ester **13** to form the triazole ring. The 3,5-dibromo-4-methylbenzylhydrazine **8** was formed in three steps from 3,5-dibromo-4-methylbenzoic acid **5**. In the first step **5** was transformed by reduction with borane−tetrahydrofuran complex into the benzyl alcohol **6** in an excellent yield of 94%. The benzyl alcohol **6** was converted into benzyl bromide **7** by treatment with phosphorus tribromide at 90 °C in a 96% yield. The benzyl bromide **7** was stored as the advanced intermediate with **8** being formed immediately prior to the reaction to form the triazole ring. For the phenyl part of the eventual ligand, we chose methyl 4-fluoro-3-iodobenzoate **9** as the starting material.[15] **9** was reacted with 4-bromo-2,5-dimethylphenylboronic acid at 66 °C under Suzuki reaction conditions to give **10** in an isolated yield of 87%. Ester **10** was then saponified to benzoic acid **11** in a 97% yield by treatment with aqueous lithium hydroxide in a methanol/tetrahydrofuran mixture heated at reflux. Acid chloride **12** was obtained by heating **11** with excess thionyl chloride, and this was directly converted into the butanimidic acid ethyl ester **13** by reacting with ethyl butyrimidate hydrochloride in the presence of triethylamine at room temperature. **13** was then used immediately in the cyclization reaction to form the triazole ring. Benzylhydrazine **8** was formed from **7** using hydrazine monohydrate, and then cyclization of benzylhydrazine **8** with the preformed acid ester **13** gave the corresponding tribrominated triazole ligand **19** in an isolated yield of 73% for the three steps with respect to **11**.

To prepare the first generation boronic acid focused twisted biphenyl dendron **18**, we used 1,3-dibromo-2-methyl-5-nitrobenzene **14** as the starting material. **14** was initially reacted with ∼2.7 equiv of 4-(2-ethylhexyloxyl)phenylboronic acid at reflux for 60 h under Suzuki reaction conditions. The coupling was found to be sluggish, and under these conditions, a mixture of **15** and some of the monosubstituted derivative were formed. The reaction could be driven to completion by using a further ∼0.46 equiv of 4-(2-ethylhexyloxyl)phenylboronic acid under the same Suzuki coupling conditions to give the desired first generation nitro-focused dendron **15** in an overall yield of 96%. The nitro group of **15** was then reduced to the corresponding amine **16** using palladium on carbon and hydrogen in a 93% yield. The amine group at the focus of **16** could then be smoothly converted into the iodo derivative **17** in a 75% yield via diazotization and reaction with potassium iodide in the presence of urea.[16]

With the two key precursor materials in hand, the final steps to prepare the doubly dendronized ligand **20** involved conversion of **17** into the boronic acid **18** and subsequent Suzuki reactions with **19**. Boronic acid **18** was formed by metalation of **17** with *tert*-butyllithium, followed by reaction with tri(*n*-butyl)borate at −78 °C, and subsequent hydrolysis with aqueous hydrochloric

Scheme 1[a]

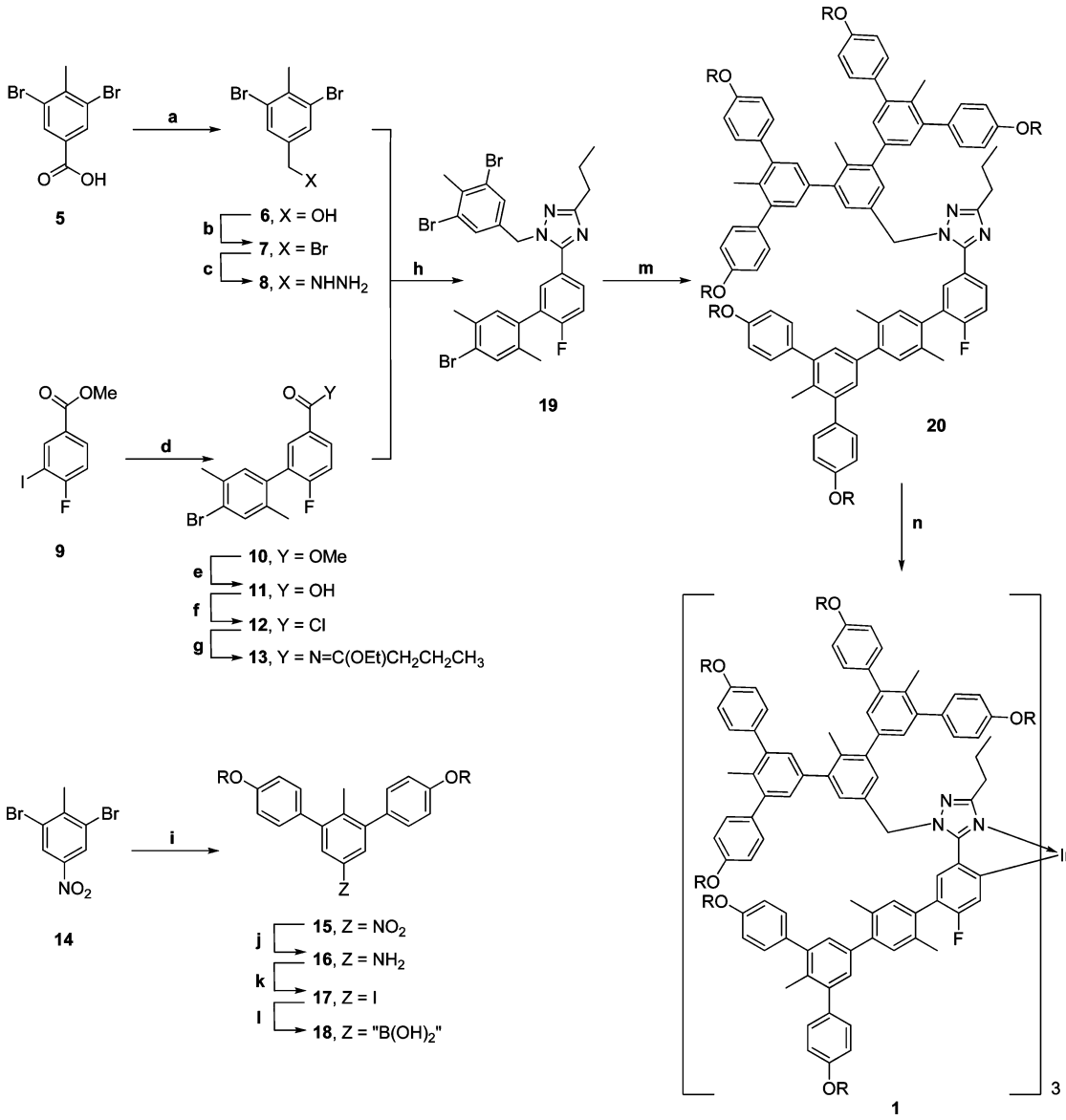

[a] Conditions and reagents: a. Borane−tetrahydrofuran complex, THF, 0−2 °C to r.t., $Ar_{(g)}$, and then ice, 94%. b. Phosphorus tribromide, heat, $Ar_{(g)}$, 96%. c. Hydrazine monohydrate, EtOH, heat, $Ar_{(g)}$. d. 4-Bromo-2,5-dimethylphenylboronic acid, $Pd(PPh_3)_4$, 2 M $Na_2CO_{3(aq)}$, MeOH, toluene, heat, $Ar_{(g)}$, 87%. e. Lithium hydroxide, water, MeOH, THF, heat, $Ar_{(g)}$, 97%. f. Thionyl chloride, heat, $Ar_{(g)}$. g. Ethyl butyrimidate hydrochloride, NEt_3, CH_2Cl_2, r.t., $Ar_{(g)}$. h. **8** and **13**, $CHCl_3$, r.t., $Ar_{(g)}$, 73% with respect to **11**. i. 4-(2-Ethylhexyloxy)phenylboronic acid, $Pd(PPh_3)_4$, 2 M $Na_2CO_{3(aq)}$, EtOH, toluene, heat, $Ar_{(g)}$, 96%. j. 10% Palladium on carbon, ethyl acetate and methanol, r.t., $H_{2(g)}$, 93%. k. Sodium nitrite, water, CH_2Cl_2, H_2SO_4, water, 0−2 °C, then urea, and then KI, water, 0−2 °C to r.t., 75%. l. *tert*-Butyllithium, THF, −78 °C, $Ar_{(g)}$, then tri(*n*-butyl)borate −78 °C and then 3 M $HCl_{(aq)}$, −78 °C to r.t. m. **18**, $Pd(PPh_3)_4$, 2 M $Na_2CO_{3(aq)}$, EtOH, toluene, heat, $Ar_{(g)}$, 98% with respect to **19**. n. Iridium(III) chloride trihydrate, water, 2-(*n*-butoxy)ethanol, heat, $Ar_{(g)}$, and then silver trifluoromethanesulfonate, **20**, diglyme, heat, $Ar_{(g)}$, 64% (R = 2-ethylhexyl).

acid. Excess **18** was then reacted with **19** under standard Suzuki conditions to give **20** in an excellent yield of 98% based on **19**.

The final step in the synthesis of dendrimer **1** was the complexation of the 'doubly dendronized' ligand **20** with 'iridium(III)'. This was achieved by following the standard two-step procedure.[10] First, **20** was reacted with iridium(III) chloride trihydrate in a water/2-(*n*-butoxy)ethanol mixture heated at reflux, and then the intermediate chloro-bridged dimer was reacted with an excess of ligand **20** in the presence of silver trifluoromethane sulfonate in diglyme at high temperature. Under these conditions, dendrimer **1** was formed in a good yield of 64% for the two steps after purification by column chromatography. As shown in Figure 2, the isotopic pattern observed in the MALDI-TOF mass spectrum was consistent with the calculated molecular weight distribution for **1**. The ^{1}H NMR spectrum of **1** displayed one simple set of ligand signals indicating that only one isomer of the core complex had formed. The iridium(III) complex at the core was assigned as the *facial* isomer by analogy to the core complex **2** for which a crystal structure has been obtained.[8] Further evidence for there being only a single isomer came from the ^{19}F NMR spectrum in which only one ^{19}F signal was observed.

The dispersity and size of the doubly dendronized ligand **20** and dendrimer **1** were investigated using gel permeation chromatography (GPC) against polystyrene standards. Both the dendronized ligand and dendrimer were found to be monodis-

(16) Endres, A.; Maas, G. *Tetrahedron* **2002**, *58*, 3999.

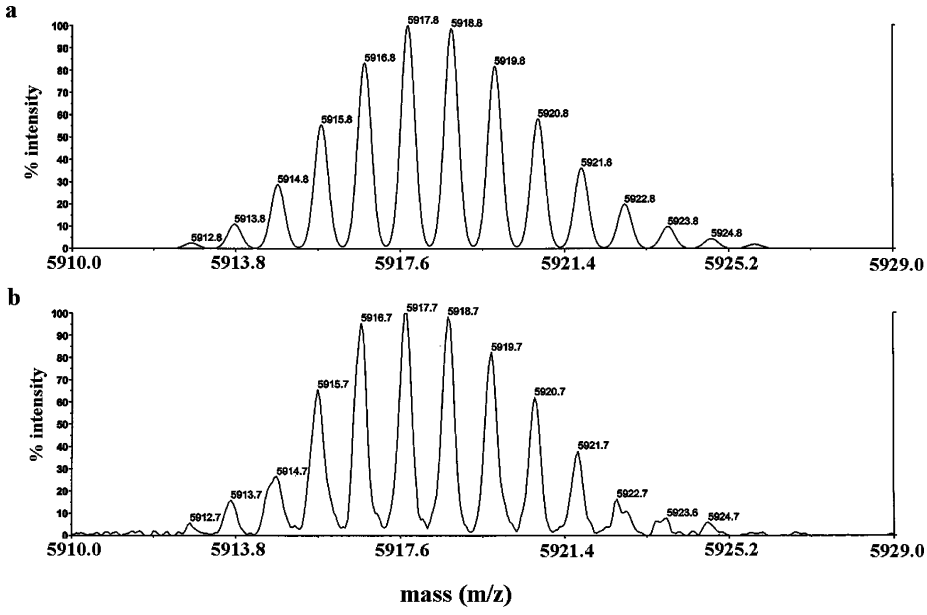

Figure 2. Parent peak of the MALDI-TOF mass spectrum of dendrimer **1** (a. calculated isotopic distribution; b. observed distribution).

Table 1. Summary of the Properties of the Iridium(III) Complex **2** and Dendrimers **1**, **3**, and **4**

	solution[a]						film[b]							
	peaks (nm)	CIEs (*x*,*y*)	PLQY (%)	τ (μs)	k_r ($\times 10^5$ s^{-1})	k_{nr} ($\times 10^5$ s^{-1})	Peaks (nm)	CIEs (*x*,*y*)	PLQY (%)	τ (μs)	k_r ($\times 10^5$ s^{-1})	k_{nr} ($\times 10^5$ s^{-1})	T_g (°C)	$E_{1/2}$ (ox)[c] (V)
2[8]	428, 456	(0.16, 0.13)	27	1.25	2.2	5.8	460	(0.17, 0.19)	18	–	–	–	–	0.50
3[14]	441, 468	(0.15, 0.16)	59	22	0.27	0.19	443, 467	(0.19, 0.22)	17	–	–	–	75	0.53
4[15]	441, 470	(0.16, 0.18)	45	1.65	2.7	3.3	441, 469	(0.16, 0.19)	49	2.1	2.3	2.4	–3	0.45
1	435, 465	(0.16, 0.16)	94	3.6	2.6	0.17	438, 466	(0.16, 0.16)	60	2.8	2.1	1.4	148	0.61

[a] Measured in toluene. [b] Spin-coated from dichloromethane solution. [c] Quoted against the ferricenium/ferrocene couple.

perse. The hydrodynamic radii of the dendronized ligand **20** and dendrimer **1** were determined from the $\bar{M}_v$s given by GPC in combination with the Hester−Mitchell equation and Mark−Houwink relationship.[17] Ligand **20** and iridium(III) dendrimer **1** had $\bar{M}_v$s of 2542 and 4528 with corresponding hydrodynamic radii of 10.9 and 15.2 Å, respectively. The hydrodynamic radius of **1** is larger than those for dendrimers **3** (biphenyl)[14] and **4** (diphenylethylene)[15] (Figure 1), which have hydrodynamic radii of 12.8 and 13.8 Å, respectively. The larger size of **1** is due to the fact that it contains one first-generation (attached via a xylyl group) and one second-generation dendron while **3** and **4** only have two first generation dendrons per ligand.

Thermogravimetric analysis (TGA) and differential scanning calorimetry were used to determine the thermal properties of dendrimer **1**. TGA indicated that dendrimer **1** had good thermal stability with a decomposition temperature, corresponding to a 5% weight loss, at 417 °C. Importantly, dendrimer **1** was found to have a glass transition (T_g) at 148 °C using a scan-rate of 300 °C/min. In contrast dendrimers **3** and **4** had the much lower T_gs of 75 °C[14] and −3 °C,[15] respectively. Dendrimer **4** has a low T_g due to the surface groups and flexible 1,2-diphenylethylene dendrons. By moving to the more rigid dendrimer **3** with biphenyl dendrons, the T_g is increased. In the case of **1** the twisted biphenyl dendrons are more rigid (less rotation around the biphenyl bonds), and this coupled with the use of a second-generation dendron[10] leads to the high T_g, which is suitable for device fabrication. These results clearly indicate that for designing light-emitting dendrimers, it is important to control the ratio of flexible to nonflexible units. Dendrimer **1** also showed excellent solubility in common organic solvents and good-quality thin films could be prepared by spin-coating.

Photophysical and Electronic Properties. We first investigated the effect of the twisted biphenyl dendrons on the electronic properties of the core complex. The electronic properties of **1** were investigated with cyclic voltammetry at a scan rate of 40 mV s^{-1}. As for the parent complex **2**,[8] we were able to observe a chemically reversible one-electron oxidation for **1** (Table 1). The key point to note from the electrochemical studies is that the $E_{1/2}$ for the oxidation of **1** (0.61 V) was similar to that of the core, indicating that the electroactive component of the dendrimer is the emissive core. The oxidation of **1** occurs at a slightly more positive potential than that of **4**,[15] reflecting the different electronic effects of the alkyl and xylyl moieties.

The UV−visible absorption spectra of dendrimers **1**, **3** (with simple biphenyl dendrons), and **4** (with phenylethylene dendrons), and their parent small molecule iridium(III) complex **2**, are shown in Figure 3. For iridium(III) complexes, the absorption spectra can be divided into two regions: the longer wavelength (>280 nm) absorptions are associated with a mixture of singlet and triplet 'metal-to-ligand'-like transitions while the absorptions in the shorter wavelength region are primarily due to the singlet $\pi-\pi^*$ transitions of the ligands (see spectrum of **2** in Figure 3). Dendrimer **1** has a peak with a high molar extinction coefficient at around 256 nm that is mainly due to the $\pi-\pi^*$ transitions of the chromophores within the dendrons. The peak

(17) Burn, P. L.; Beavington, R.; Frampton, M. J.; Pillow, J. N. G.; Halim, M.; Lupton, J. M.; Samuel, I. D. W. *Mater. Sci. Eng., B* **2001**, *85*, 190.

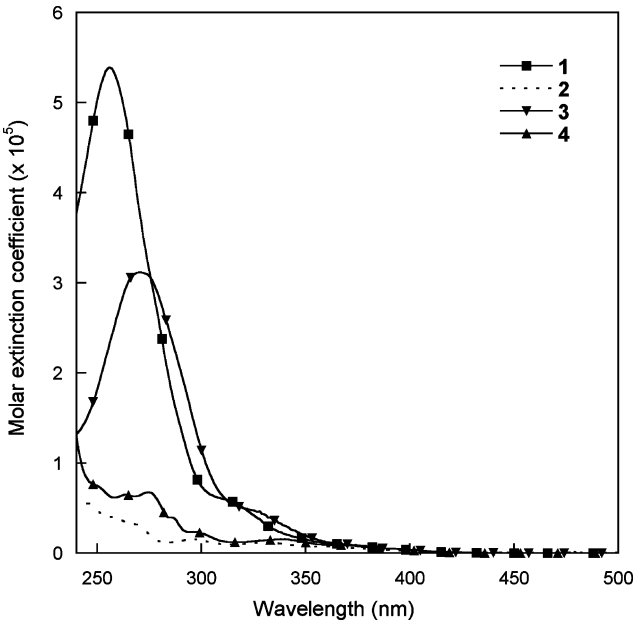

Figure 3. Solution UV−visible spectra for **1**−**4** in dichloromethane.

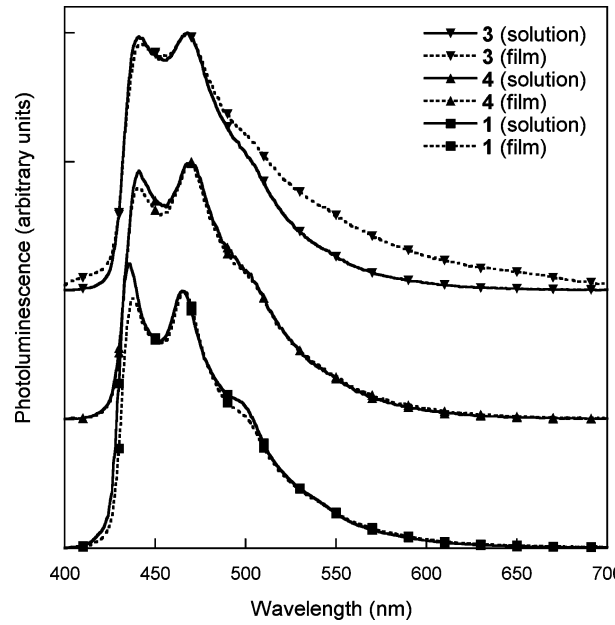

Figure 4. Solution and film photoluminescence spectra for **1**, **3**, and **4**. The spectra have been normalized and offset for comparison (the excitation wavelength is 360 nm for solution and 325 nm for film).

absorption for the biphenyl dendrons of **3** is at 271 nm, which is red-shifted compared to **1** due to biphenyl dendrons being able to adopt a more planar arrangement. The dendron absorption of **4** at around 270 nm is much weaker due to the phenyl rings being isolated chromophores.

The next step in the study was to see whether the rigid dendrons had a positive effect on the emissive properties of the phosphorescent core complex. The solution and film PL spectra of **1**, **3**, and **4** are shown in Figure 4 and the emissive properties summarized in Table 1. The parent complex core **2** has a solution photoluminescence quantum yield (PLQY) of 27% at room temperature, CIE coordinates of (0.16, 0.13), and a photoluminescence (PL) lifetime of 1.25 μs. A PL lifetime of 1.25 μs is consistent with phosphorescence associated with a ligand-to-metal charge transfer type emission. It is important to note that the relatively low PLQY of **2** is due to a relatively large nonradiative decay rate, which has been attributed to strong vibrational coupling.[18] We have observed that attachment of biphenyl-based dendrons can increase the PLQY of simple complexes, and this may be in part due to the large group decreasing the vibrational modes that lead to the quenching of the luminescence. For example, attachment of biphenyl-based dendrons to **2** to give **3** was found to increase the solution PLQY from 27% to 59% with little change in the emission color. However, the addition did cause a large change in the PL lifetime, with it increasing from 1.25 μs for **2** to 22 μs for **3**. The increase in PL lifetime is due to the core and the dendrons having similar triplet energies allowing the triplet excitons to spend time on the dendrons although emission still occurs from the complex at the core. The fact that the triplet exciton could reside on the dendrons of **3** meant that there was a dramatic drop in the solid-state PLQY, which fell to 17%.[14] By replacing the biphenyl dendrons of **3** with the 1,2-diphenylethylene dendrons of **4** it proved possible to confine the triplet exciton on the core of the dendrimer.[15] Dendrimer **4** had a respectable solution PLQY of 45% and a PL lifetime of 1.65 μs with the latter indicating emission from the core complex. The remarkable feature of the emissive properties of **4** was that in the solid-state the PLQY remained a creditable 49% although the CIE coordinates were less blue.

Dendrimer **1** has a solution PLQY of 94%, which is over three times that of the core complex. The PL lifetime of 3.6 μs indicates that the emission is phosphorescent in nature and due to the core. This shows that the twisting of the biphenyl units in the dendrons raises their singlet and triplet energies such that the excited state is localized on the core complex. The radiative decay rates of **1** and **2** are the same, and hence the improvement in PLQY is primarily due to the dramatic reduction in the nonradiative decay rate for **1** (Table 1). We attribute the reduced non-radiative decay rate to the rigidifying effect of the dendrons which reduces the geometry change in the excited state, and hence also the amount of vibrational quenching. The strong weighting of the (0,0) transition in the solution PL and the lack of red tail in the film PL give rise to the good blue emission from **1**. Importantly, the attachment of the 'twisted' biphenyl-based dendrons has not changed the color of the emission appreciably with the CIE coordinates of **1** being (0.16, 0.16) versus (0.16, 0.13) for **2**. Interestingly, in forming films of **2** (the unadorned complex) the color of the emission changes notably with CIE coordinates of (0.17, 0.19). In contrast, the emission color of **1** remains essentially unchanged with the peaks of the emission within a few nanometers and the CIE coordinates being (0.16, 0.16). The fact that the color has not changed suggests that the intermolecular interactions that lead to aggregate or excimer emission have been controlled. This can be understood by considering the arrangement of the dendrons around the core complex. The core iridium(III) complex is the *facial* isomer, and hence having dendrons on each of the aromatic rings of all the ligands means that the core is encapsulated by the dendrons. This is reflected in the hydrodynamic radii of **1**, which is the largest of all three dendrimers shown here. The hydrodynamic radius of **4** is larger than that of **3** due to the extension of the dendrons caused by the linking 1,2-diphenylethylene units. For **1**, the radius (15.2 Å) is larger still, due to the fact that the dendron on the triazolyl

(18) Harding, R. E.; Lo, S.-C.; Shipley, C. P.; Burn, P. L.; Samuel, I. D. W. *Org. Electron.* **2008**, *9*, 377.

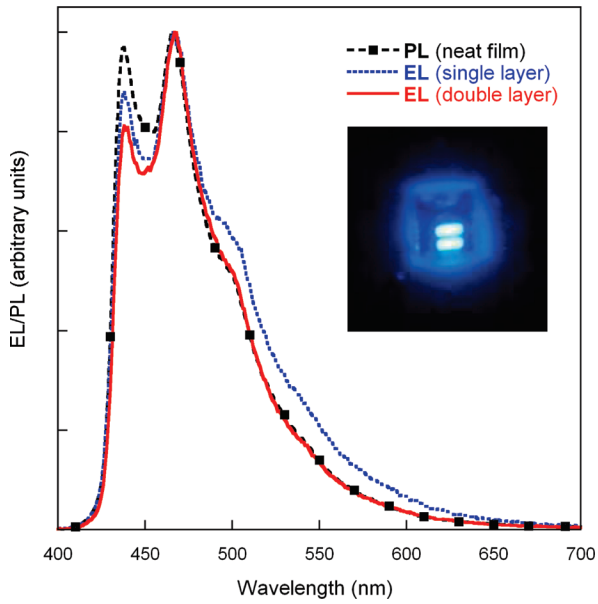

Figure 5. Film PL spectrum for dendrimer **1** and EL spectra of the single (ITO/dendrimer **1**/Ca:Al) and bilayer (ITO/dendrimer **1**/PBD/LiF:Al) devices. The inset is a photo of the single layer device.

ring is second-generation and the first-generation dendron is linked to the ligand phenyl ring via another phenyl moiety. The benefit of encapsulating the emissive core well can be seen in the solid-state PLQY of **1**, which at 60% is very high for a material that emits saturated blue phosphorescence. The lower solid-state PLQY is primarily due to a larger nonradiative decay rate. Large nonradiative decay rates in this family of iridium(III) complexes has been attributed to enhanced coupling of the excited state to vibrational modes,[18] which is exhibited by an increase in the strength of the (0,1) to the (0,0) transition. It can be seen that for **1** there is a change in the ratio of the (0,1) to (0,0) transition in going from solution to the solid-state with the (0,1) transition being larger in the film (Figure 4). This suggests that there is stronger coupling of the excited state and vibrational modes for **1** in the solid-state than in solution, which could arise from the packing of the dendrimer in the film causing a slightly different conformation.

Organic Light-Emitting Diodes. Given that **1** can be spin-coated to form good quality thin films that are morphologically stable, simple OLEDs were fabricated. The device performance is summarized here with the full characteristics shown in the Supporting Information. We first fabricated a single layer device with an indium tin oxide (ITO) anode and calcium cathode [ITO/dendrimer **1** (100 nm)/Ca/Al]. The color of the emission was blue (see inset of Figure 5) with CIE coordinates of (0.17, 0.20). Although the blue color is very good, the small reduction in color saturation for the EL spectrum versus the film PL is due to a difference in weighting of the (0,0), (0,1), and (0,2) transitions and an increase in the emission at longer wavelengths. At 100 cd/m^2 the device had an external quantum efficiency of 0.41% at 26.7 V, giving power and luminous efficiencies of 0.08 lm/W and 0.65 cd/A, respectively. The high voltage and increasing efficiency at increasing bias (see Supporting Information) indicate that large barriers to charge injection limited the efficiency. The work function of oxygen plasma-treated ITO is around 4.8 eV[19] depending on its pretreatment while calcium

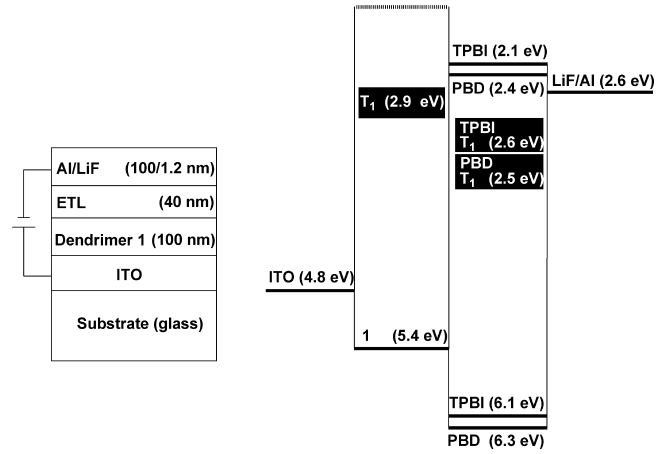

Figure 6. Bilayer device structure and energy level diagram for the materials showing HOMO, LUMO, and triplet energies (T_1).

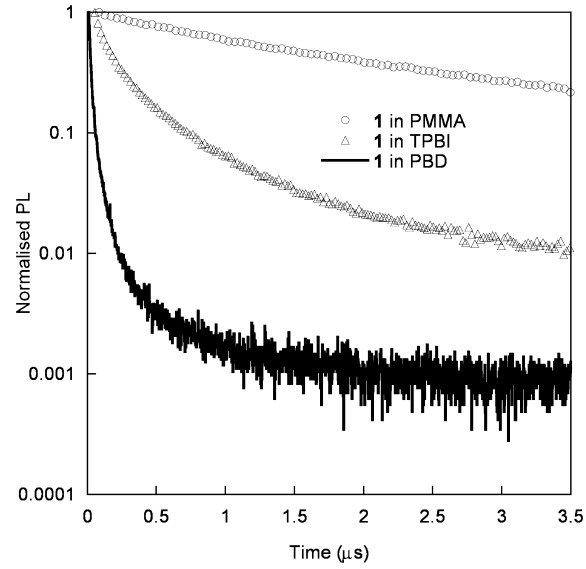

Figure 7. Time-resolved PL of films of dendrimer **1** in PMMA, TPBI, or PBD. Excitation = 393 nm.

has a work function of 2.9 eV. To gain an understanding of the barriers to charge injection (summarized in Figure 6), we calculated the Highest Occupied Molecular Orbital (HOMO) energy level to be 5.4 eV from the $E_{1/2}$ for the oxidation (0.61 V against the ferrocenium/ferrocene couple) given that the ionization potential of ferrocence is 4.8 eV,[20] and the Lowest Unoccupied Molecular Orbital (LUMO) energy of 2.2 eV was then estimated by adding the singlet energy of 3.2 eV of the core complex[8] to the HOMO energy level.

In previous work on OLEDs containing phosphorescent dendrimers the device efficiency was found to be high when an electron transporting hole blocking layer was used.[13,14,21] Therefore, in order to improve electron injection into the devices we prepared bilayer OLEDs with a neat film of dendrimer **1** and an electron transport layer (ETL) of either 1,3,5-tris(2-*N*-phenylbenzimidazolyl)benzene (TPBI) or 2-(4-biphenyl)-5-(4-

(19) Kim, K.-P.; Hussain, A. M.; Hwang, D.-K.; Woo, S.-H.; Lyu, H.-K.; Baek, S.-H.; Jang, Y.; Kim, J.-H. *Jpn. J. Appl. Phys.* **2009**, *48*, 021601.

(20) D'Andrade, B. W.; Datta, S.; Forrest, S. R.; Djurovich, P.; Polikarpov, E.; Thompson, M. E. *Org. Electron.* **2005**, *6*, 11.

(21) (a) Lo, S.-C.; Male, N. A. H.; Markham, J. P. J.; Magennis, S. W.; Burn, P. L.; Salata, O. V.; Samuel, I. D. W. *Adv. Mater.* **2002**, *14*, 975. (b) Anthopoulos, T. D.; Frampton, M. J.; Namdas, E. B.; Burn, P. L.; Samuel, I. D. W. *Adv. Mater.* **2004**, *16*, 557.

tert-butylphenyl)-1,3,4-oxadiazole (PBD) (ITO/dendrimer **1**/ETL/LiF/Al). For the devices with TPBI, the quantum efficiency increased with increasing voltage, and at 18 V a brightness of 100 cd/m^2 was obtained with an EQE of 2.2% (0.46 lm/W, 2.6 cd/A). For PBD, the EQE was highest at low brightness and decreased as the voltage increased. The maximum external quantum efficiency (EQE) was 3.9% (5.0 V, 3.4 lm/W, 5.4 cd/A) and at a brightness of 100 cd/m^2 the EQE was 2.1% (15.0 V, 0.61 lm/W, 2.9 cd/A). The EL spectrum (Figure 5) shows deep blue emission was improved relative to the single layer device and the CIE coordinates of (0.16, 0.17) are very close to the PL coordinates of (0.16, 0.16). The EQE of 2.1% at 100 cd/m^2 is very good for such a simple device structure and not too far from the efficiencies at comparable brightnesses (≈8% at 100 cd/m^2) reported for much more complex state-of-the-art deep blue phosphorescent devices.[22] These latter devices are prepared by evaporation and contain seven layers and six compounds in contrast to the two layers and two materials of this work. The improved performance of the bilayer devices arises from better charge balance due to the electron transporting and hole blocking action of the ETLs. LiF-Al has a work function of 2.6 eV,[23] TPBI has a reduction potential of 2.7 V versus the ferrocenium/ferrocene couple, which corresponds to a LUMO energy of approximately 2.1 eV (based on ferrocene having an ionization potential of 4.8 eV[20]), and PBD has a LUMO of energy of 2.4 eV[24] (see Figure 6). This means that there is still a substantial barrier to electron injection in the TPBI device, which explains its higher operating voltage than the PBD device. The relatively high operating voltage of both devices is also likely to be due to the remaining substantial barrier to hole injection.

The external quantum efficiency of the devices is less than might be expected from a film with a PLQY of 60%. One potential reason for the lower EQEs in the bilayer devices is that excitons will be formed near the dendrimer:ETL interface and could then be quenched by the ETL. It has been reported that the triplet energies for TPBI and PBD are 2.6 eV[25] and 2.5 eV,[26] respectively, which is lower than the emission energy of dendrimer **1**. To probe whether this is indeed a factor, we compared the PL lifetime of emission from dendrimer **1** in blends with poly(methylmethacrylate) (PMMA, used as an inert host), TPBI, and PBD (Figure 7). It can be readily seen that the PL decays much faster in the blends with TPBI and PBD. The time for the emission to fall to 1/e of its initial value is 2.18 μs in PMMA, 0.23 μs in TPBI, and 0.024 μs in PBD. The shortened lifetime indicates that the ETLs quench the luminescence of the dendrimer.

Clearly both the barrier to hole injection and quenching of the EL by the ETL are limiting device performance. Therefore, to improve the efficiency of the devices, a hole-injection layer (which is insoluble in the dendrimer processing solvent) needs to be included. In addition, the hole and electron transport layers will have to have triplet energies higher than that of the emissive layer to enable solution processed deep blue phosphorescent dendrimers to give optimum performance in an OLED.

Conclusion

In conclusion, we have shown that dendrimers provide a route to solution-processable saturated blue phosphorescent materials with a high solid-state photoluminescence quantum yield and promise for OLEDs. This advance has been achieved by the use of new high triplet energy 'twisted' dendrons that can be used to confine the excited state on a blue emissive phosphorescent core. This new family of dendrons was found to significantly reduce the nonradiative decay rate while leaving the radiative decay rate essentially unchanged, leading to a blue phosphorescent dendrimer with the exceptionally high solution PLQY of 94% at room temperature. The film PLQY of 60% with CIE coordinates of (0.16, 0.16) means that the dendrimer is an excellent candidate for OLEDs. Preliminary devices indicate that good efficiencies can be achieved, and the next steps are the design of hole and electron transport materials with suitable triplet energies.

Acknowledgment. This work was supported by CDT Oxford Ltd and the EPSRC. Professor Paul L. Burn is recipient of an Australian Research Council Federation Fellowship (project number FF0668728). Professor Ifor Samuel holds an EPSRC Senior Research Fellowship (grant number EP/C542398).

Supporting Information Available: Experimental procedures, spectral data for compounds, and device characteristics. This material is available free of charge via the Internet at http://pubs.acs.org.

JA903157E

(22) Chiu, Y.-C.; Hung, J.-Y.; Chi, Y.; Chen, C.-C.; Chang, C.-H.; Wu, C.-C.; Cheng, Y.-M.; Yu, Y.-C.; Lee, G.-H.; Chou, P.-T. *Adv. Mater.* **2009**, *21*, 2221.
(23) Hung, L. S.; Tang, C. W.; Mason, M. G.; Raychaudhuri, P.; Madathil, J. *Appl. Phys. Lett.* **2001**, *78*, 544.
(24) Janietz, S.; Wedel, A. *Adv. Mater.* **1997**, *9*, 403.
(25) Fukagawa, H.; Watanabe, K.; Tokito, S. *Org. Electron.* **2009**, *10*, 798.
(26) Suzuki, M.; Tokito, S.; Sato, F.; Igarashi, T.; Kondo, K.; Koyama, T.; Yamaguchi, T. *Appl. Phys. Lett.* **2005**, *86*, 103507.